Observation and modelling of shear-band propagation in glassy polycarbonate

J. Grenet* and C. G'Sell†
Laboratoire de Physique du Solide (UA CNRS DO 155), Ecole Nationale Supérieure des Mines, INPL, Parc de Saurupt, 54042 Nancy Cedex, France
(Received 14 August 1989; accepted 14 November 1989)

Plane simple shear tests were performed on polycarbonate specimens with a miniaturized shearing machine installed on the stage of a scanning electron microscope. The *in situ* observations show the nucleation and growth (longitudinal and transverse) of a unique shear band. From measurements of the band length, of the band width and of the local shear during the course of the test, the kinetics of this plastic instability were specially analysed.

In addition, a computer simulation of band propagation was achieved. It is based on (i) the intrinsic constitutive equation of the material and (ii) the two-dimensional internal stress field generated by the shear gradient. The simulation takes into account correctly the different stages of the test including the formation and the propagation of the band. In particular, it appears that the lateral widening of the band is controlled by internal stresses which were initiated on the band fronts during the longitudinal propagation phase.

(Keywords: polycarbonate; shear; modelling)

INTRODUCTION

After a number of experimental pieces of evidence published in the literature, it is now widely acknowledged that glassy polymers exhibit plastic deformation below T_g (glass transition temperature) mainly through the activation of shear bands. Among other polymers, bisphenol-A polycarbonate (PC) revealed itself as a very interesting polymer for the study of the shear-banding mechanism due to its remarkable toughness favoured by low-temperature relaxation capabilities[1]. Because of this particular feature, PC deforms plastically without critical crazing over a large range of temperature below T_g and under various types of loading: tension[2], compression[3] and simple shear[4,5].

Most observations were reported from uniaxial tension and compression experiments, where the bands developed obliquely to the loading axis. They were generally initiated in stress-concentration zones (scratches, notches, etc.) and then propagated into the bulk, while the recorded stress–strain curve displayed a marked yield drop. In these tests, the bands multiply along two or more shearing directions, according to the geometry of the specimens and the boundary conditions[6]. In most experiments the development of the bands was difficult to analyse quantitatively because of its great instability under the effect of the elastic energy stored during the loading sequence and because of the interactions between bands propagating along different shear directions[7].

In this effort towards a closer understanding of the plastic banding mechanisms, simple shear experiments are of outstanding interest since they favour a unique shear plane and thus avoid the problem of band crossing. By means of torsion tests, it was shown[5] that isolated shear bands could be initiated and grown at will in PC cylindrical test-pieces and even reverted back to zero strain by application of a negative torque. However, because the torque vs. twist curves could not be simply resolved in terms of shear stress vs. shear strain behaviour[8], the interpretation of the tests remained at a qualitative level. More recently, it was found in this laboratory[9] that the plane simple shear test was more favourable for the study of shear-banding kinetics since, like torsion, it allows the initiation of a unique shear band in the sample and, furthermore, it is better adapted to the determination of shear stress and shear strain inside the growing band.

The aim of the present work was twofold: (i) first, to illustrate the capabilities of the latter experimental technique by correlating the main steps of shear-band propagation with the intrinsic constitutive behaviour of polycarbonate; and (ii) secondly, to describe in some detail the driving forces that promote the longitudinal and transverse propagation of a shear band, in terms of micromechanical and macromolecular mechanisms. This analysis will provide the ingredients of a finite-difference computation for the modelling of the entire banding process on the basis of the shear stress vs. shear strain behaviour of the polymer.

EXPERIMENTAL INVESTIGATION

Specimens

Shear specimens were machined out of the same plates of Makrolon polycarbonate as in previous studies[4,10]. This amorphous thermoplastic polymer was characterized by its average molecular weight $\bar{M}_w = 28\,800\,g\,mol^{-1}$, its polydispersity $\bar{M}_w/\bar{M}_n = 1.85$ and its glass transition temperature $T_g = 145°C$. The shape of the samples is indicated in *Figure 1*. The dimensions of the calibrated part are: length $L = 60\,mm$, width $h = 4\,mm$ and thickness

* On leave from: Faculté des Sciences de Rouen, Laboratoire LECAP, BP 118, 76134 Mont-Saint-Aignan Cedex, France
† To whom correspondence should be addressed

0032-3861/90/112057-09

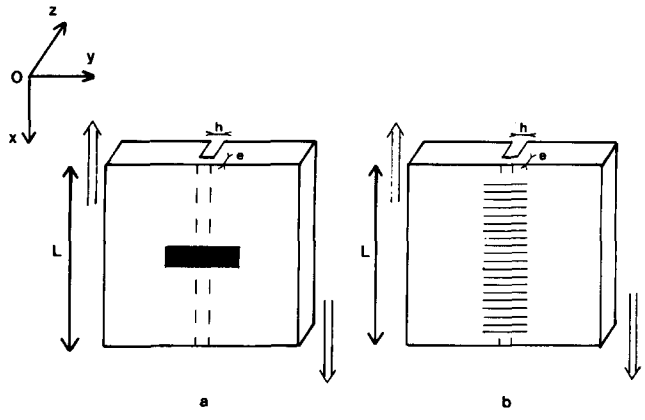

Figure 1 Polycarbonate samples used for the shear tests with: (a) a centrally printed marker; (b) an array of engraved parallel markers

$e=3$ mm or 1 mm. The massive heads on both sides are designed to be gripped in the jaws of the shearing stage.

Two types of markers were used to monitor the local shear in the course of the tests. In the first type (*Figure 1a*), the flat surface of the specimen was simply marked, in its central part, with a straight line printed with a strongly adherent and flexible ink. This marking system was used for the determination of the constitutive behaviour of the material. In the second type (*Figure 1b*), a fine array of parallel lines was lightly engraved on the polished specimen by means of a razor blade adapted on the arm of a computerized plotter. The spacing of the lines was equal to 0.1 mm. This array served to follow the distribution of shear strain throughout the whole calibrated area. In both cases, the current value of the local shear was determined through the relation $\gamma_{loc}=\tan\theta_{loc}$, where θ_{loc} represents the local rotation of a marker originally perpendicular to the shear direction Ox. By contrast, the applied shear γ was defined as the average value of the local shear over the whole width of the sample (it corresponds to the relative shear displacement of the gripped heads divided by the width h).

Moreover, for all specimens, a very small geometric defect was made centrally on the rear face of the calibrated portion by scraping the polymer gently with a round-tipped cutting tool. This operation resulted in reducing the thickness by about 1% in a small area. It was designed to fix the initiation locus of the eventual shear band.

Before the tests, the samples were carefully annealed in a dry oven at 110°C for 48 h in order to make them free of moisture and internal stresses. They were slowly cooled down to ambient temperature and then kept in a desiccator.

Apparent stress–strain behaviour in simple shear

Polycarbonate samples of the first type were mounted in a shear stage installed in a universal MTS testing machine and subjected to a constant applied shear rate $\dot{\gamma}=5\times10^{-4}\,s^{-1}$ at room temperature (25±1°C). The shear rate was slow enough to ensure isothermal deformation. During the course of the test, the evolution of the single ink marker was followed *in situ* by means of a video camera interfaced with a microcomputer, as described in more detail in another paper[11].

The curve in *Figure 2a* displays the evolution of the applied shear stress (shear force per unit cross section, $\tau=F/Le$) during such a simple shear test. Several deformation stages are observed, which correspond to different distortion modes of the marker (*Figure 2b*).

Stage I. Homogeneous viscoelastic response ending at the upper yield stress. The marker remains straight and simply rotates as stress increases.

Stage II. Shear stress drop associated with the initiation of plastic deformation. This concentrates in a narrow portion of the specimen width, as assessed by the kinking of the ink marker (it will be proved later that this effect corresponds to the formation of a shear band).

Stage III. Quasi-linear plateau up to $\gamma=0.8$. During this stage, the marker kink (plastic band) propagates laterally to both sides of the calibrated part.

Stage IV. Generalized plastic flow of the sample with enhanced hardening. This homogeneous deformation regime begins as soon as the propagation of the plastic zone has reached the edges of the calibrated part. The marker has recovered its straight shape and continues rotating until rupture of the specimen occurs.

Two-dimensional shear-band development

In addition to the above experiments, special tests were performed with a miniaturized shearing machine (*Figure 3*), which was specially designed to observe the detailed two-dimensional geometry of the shear band under load.

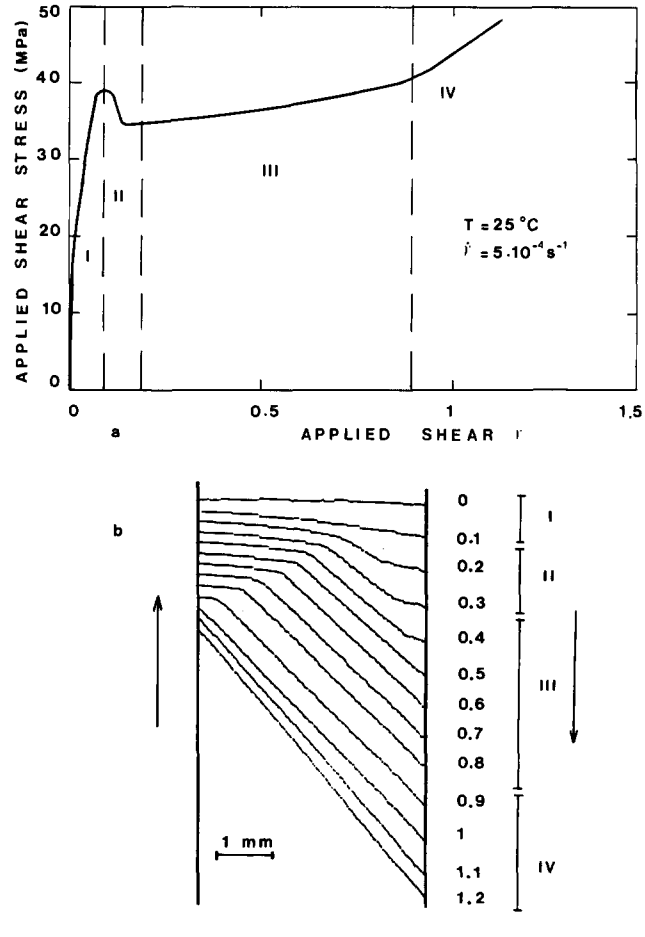

Figure 2 Apparent behaviour of polycarbonate in simple shear: (a) applied stress–applied shear curve; (b) evolution of the surface marker

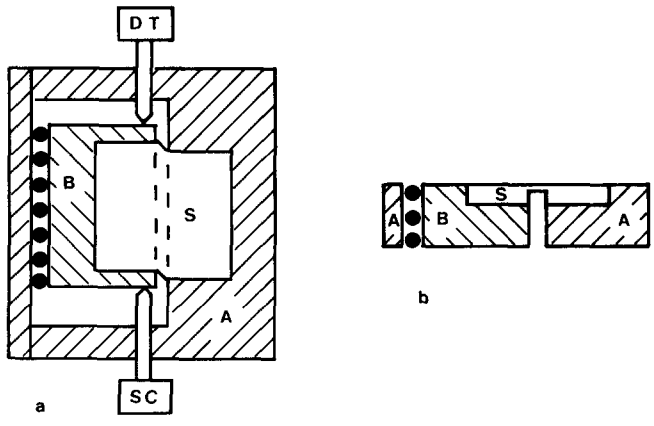

Figure 3 Schematic diagram of the miniaturized shearing machine: (a) front view; (b) end view

The dimensions ($135 \times 122\,mm^2$) and the weight (3 kg) were small enough for the machine to be installed on the stage of a scanning electron microscope. It is made of a rigid frame (A) and a mobile part (B) guided by a linear ball slider and actuated by a screw (SC). The displacement is monitored by means of a transducer (DT). The specimen heads are firmly attached to parts A and B, respectively, and deformed step by step to increasing values of the applied shear up to $\gamma_{max} = 1.4$. At each step, the sample (S) was examined microscopically while the shear was held constant.

Figure 4 illustrates the successive stages of the propagation of a shear band in a specimen of the second type, engraved with an array of fine parallel lines. The lines were originally oriented along the Oy direction. Their distortion gives access to the two-dimensional distribution of the local shear γ_{loc} at each step of the sample deformation. It should be noted now that the local shear determined by this method under stress includes both the viscoelastic and the plastic components of strain.

The microscopic observations displayed in *Figure 4* clearly concur with the different stages of the apparent strain–stress curve of *Figure 2a*.

Stage I. For an applied shear lower than the yield strain, the array deformed homogeneously by viscoelastic mechanisms (*Figure 4b* at $\gamma = 0.05$). This deformation could be recovered by unloading the sample.

Stage II. As the shear stress passes its maximum, a single band appeared at the location of the thickness defect. The micrograph in *Figure 4c* was obtained while the applied shear was equal to 0.095. The presence of a shear band parallel to Ox is assessed by the occurrence of sharp kinks on the engraved lines. The band appears more clearly if the micrograph is viewed parallel to the lines and holding the plane of the figure at eye level. It is evident that the width of the band is of the order of 0.1 mm and that it does not occupy the whole length of the specimen (the enlarged view in *Figure 5* demonstrates that the region selected contains the lower tip of the shear band). The distortion of the array of lines was analysed quantitatively in terms of the local shear γ_{loc}. Curve b in *Figure 6* shows that γ_{loc} drops rather abruptly at the band tip: over a length of 2 mm, the local shear decreases from a value of about 0.75 (in the band) down to the viscoelastic shear lower than 0.1 (ahead of the band). While the shear decreased during stage II, the parameters of the growing band were slightly modified: (i) the transition zone at the tips of the band was spread (curve c, *Figure 6*), (ii) the local shear inside the band increased somewhat and (iii) the width of the band began to grow (see curves a and b, *Figure 7*).

Stage III. The plateau stage was essentially characterized by the gradual widening of the band (*Figures 4d* and *4e*). It began when the band had reached the ends of the specimen, while the stress passed through a minimum, at $\gamma \simeq 0.2$. From the quantitative measurements (*Figure 8*) it is clear that the width of the band increases linearly with the applied shear. However, as shown in *Figure 7*, the widening was not necessarily symmetrical and could be influenced by a very slight non-uniformity in the specimen thickness. It should also be remarked that the local shear inside the band continued to increase at a very slow rate during band widening. Finally, stage III ended when the band occupied the whole calibrated part of the sample, at an applied shear $\gamma \simeq 0.9$.

Stage IV. This last stage is characterized by the homogeneous plastic deformation of the specimen, the applied shear γ being equal to the local shear γ_{loc} at any point of the sample.

Determination of the intrinsic constitutive equation of polycarbonate

The apparent stress–strain behaviour displayed in *Figure 2a* represents the mean response of the overall specimen and not the true intrinsic behaviour of a microscopic material element. In order to determine the latter, the above behaviour was reconsidered in terms of the variations of the shear stress τ *versus* the local shear γ_{loc}. The computer records of the marker shape were analysed at a number of steps during the shear test, and the local shear was measured from the local slope of the marker in the centre of the specimen (where the shear band was initiated). However, the local stress–strain curve thus obtained did not correspond to a constant local shear rate. As shown by the γ_{loc} vs. γ plot of *Figure 8*, the local shear rate $\dot{\gamma}_{loc}$ was much faster than the applied shear rate $\dot{\gamma}$ while the plastic shear localized during stage II, and $\dot{\gamma}_{loc}$ was much slower than $\dot{\gamma}$ when the band propagated laterally during stage III. The two rates match only during the homogeneous stages I and IV. In order to correct the shear stress for these shear-rate fluctuations, the following expression was used:

$$\tau(\dot{\gamma}_{ref}) = \tau(\dot{\gamma}_{loc})(\dot{\gamma}_{ref}/\dot{\gamma}_{loc})^m \qquad (1)$$

where $\dot{\gamma}_{ref}$ is a fixed reference value of the local shear rate while the strain-rate sensitivity coefficient $m = (\partial \ln \tau / \partial \ln \dot{\gamma}_{loc})_{\gamma_{loc}}$ was found to be equal to about 0.027 for polycarbonate in a previous work[4]. By means of the above procedure, the intrinsic (local) stress–strain behaviour was derived for a constant reference shear (local) rate $\dot{\gamma}_{ref} = 5 \times 10^{-4}\,s^{-1}$ and is displayed in *Figure 9*. It is evident that this curve differs from the apparent behaviour in *Figure 2a:* (i) at the yield drop, whose slope is less abrupt, and (ii) in the medium shear range, where the stress plateau is no longer observed. Instead, a gradually hardening plastic regime is recorded once the lower yield stress is passed, in contrast to the stage III–stage IV transition observed previously.

This intrinsic behaviour of glassy polycarbonate corresponds to specific mechanisms that have been proposed

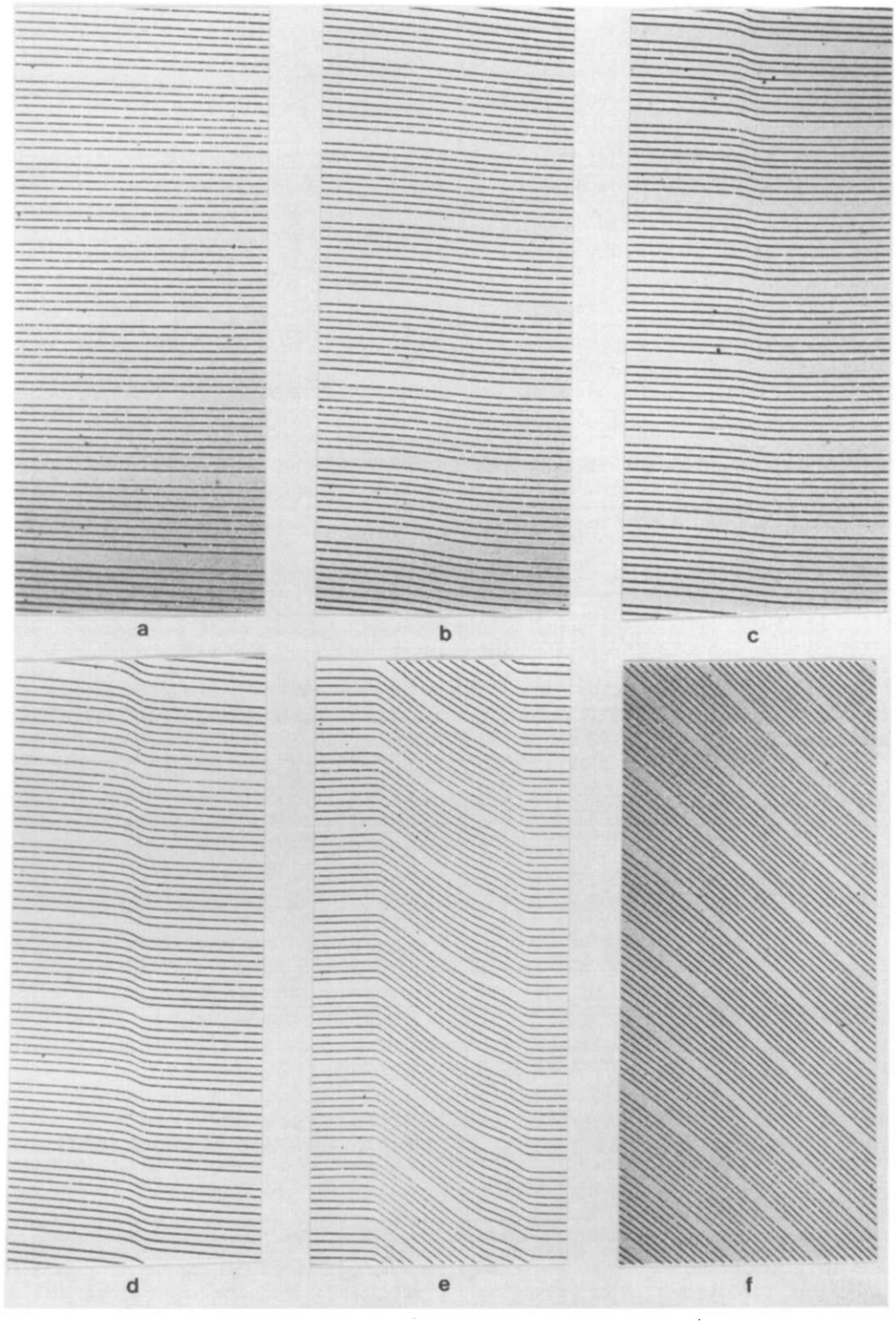

Figure 4 Distortion of the microscopic array of lines on a polycarbonate sample under simple shear: (a) $\gamma=0$; (b) $\gamma=0.05$; (c) $\gamma=0.095$; (d) $\gamma=0.12$; (e) $\gamma=0.26$; (f) $\gamma=1$

earlier[11–13]. The stress drop at yield results from an avalanche of 'defects' associated with collective conformational changes of molecules in microscopic domains, while the final strain hardening would be due to the entropic effect of the gradual orientation of the macromolecular chains[14].

It is now possible to describe the intrinsic plastic behaviour of polycarbonate by means of an appropriate constitutive equation $\tau(\gamma_{loc}, \dot{\gamma}_{loc})$ fitted with the above data. Following a previous analysis[15], we will use here the following phenomenological expression

$$\tau(\gamma_{loc}, \dot{\gamma}_{loc}) = V(\gamma_{loc})Y(\gamma_{loc})H(\gamma_{loc})(\dot{\gamma}_{loc})^m \qquad (2)$$

In this multiplicative law, the first term describes the initial viscoelastic rise:

$$V(\gamma_{loc}) = K[1-\exp(-w\gamma_{loc})]$$

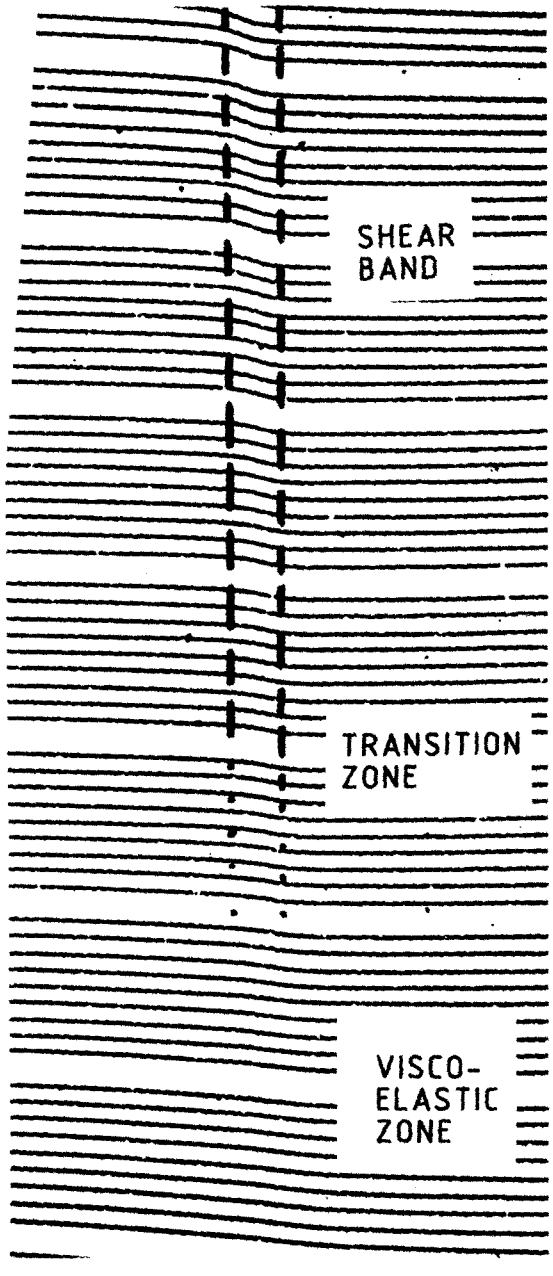

Figure 5 Enlarged view of the same band as in *Figure 4c* showing one end of the band in the course of longitudinal propagation

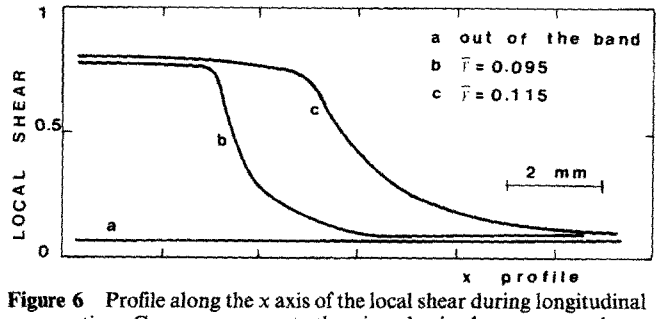

Figure 6 Profile along the x axis of the local shear during longitudinal propagation. Curve a represents the viscoelastic shear measured out of the band; curves b and c were obtained for two values of the applied shear

the second takes into account the yield drop:

$$Y(\gamma_{loc}) = 1 + a \exp(-b\gamma_{loc})$$

the third holds for strain hardening:

$$H(\gamma_{loc}) = 1 + c\gamma_{loc}$$

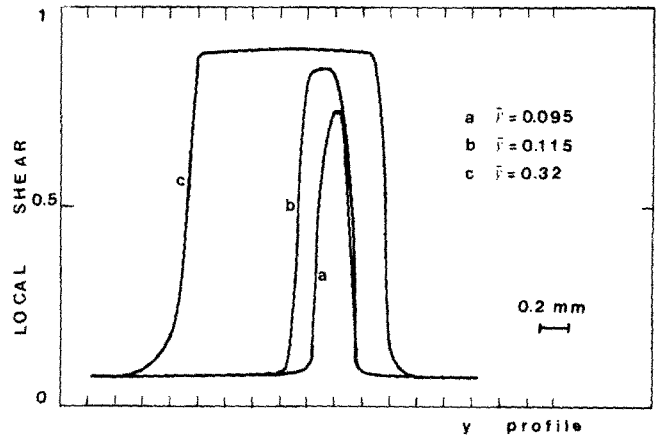

Figure 7 Profile along the y axis of the local shear during two stages of band propagation: longitudinal (curves a and b) and lateral (curve c)

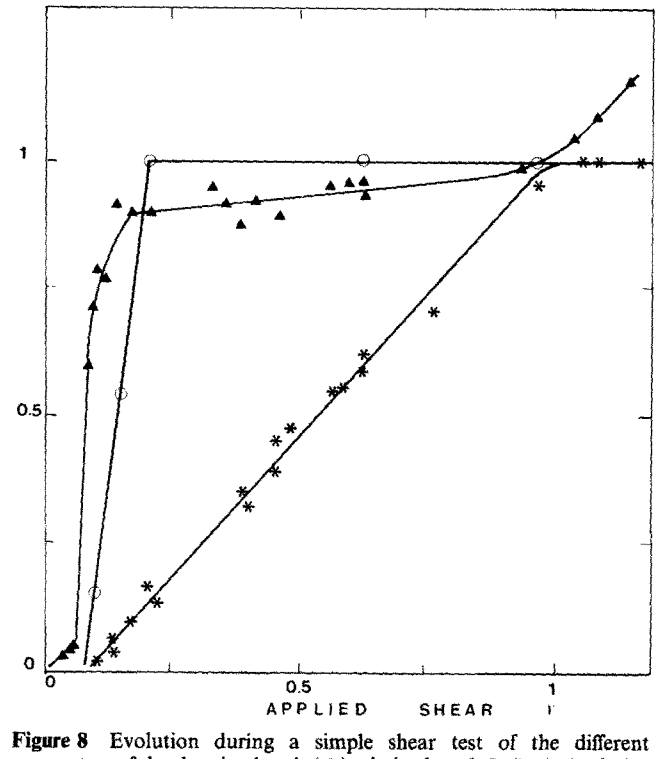

Figure 8 Evolution during a simple shear test of the different parameters of the shearing band: (○) relative length L_b/L; (✱) relative width h_b/h; (▲) local shear in the band γ_b. The applied shear includes the elastic and the plastic components

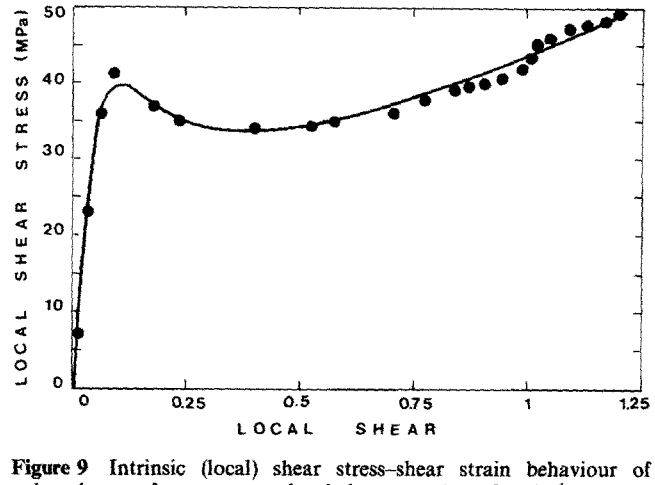

Figure 9 Intrinsic (local) shear stress–shear strain behaviour of polycarbonate for a constant local shear rate $\dot{\gamma}_{loc} = 5 \times 10^{-4}$ at 25°C. The data points were derived from the experimental record; the full curve was fitted with the constitutive equation

and the final term determines the strain-rate sensitivity. The parameters of the constitutive equation were fitted to the experiment, leading to the modelled curve displayed in *Figure 9*.

COMPUTER SIMULATION OF BAND PROPAGATION

After the experimental observations presented in the previous section, it appears clearly that the propagation of a plastic shear band in polycarbonate is an intrinsic and gradual process, in contrast to its initiation which depends essentially on the availability of geometric or structural defects[16]. An important problem is to understand what are the driving factors that control the propagation kinetics. In previous papers[4,17,18], arguments have been developed to interpret the longitudinal development of a shear band in terms of the internal stresses induced in the elastic material ahead of the tip of the elongating band. However, the steady-state lateral widening of the fully elongated band has not been discussed hitherto with the same attention. In a recent paper[18], one of the authors wondered whether or not the widening process of the band would be controlled by micromechanical factors or by the lateral diffusion of structural defects out of the plastically deformed band. The object of this section is to answer this question by reporting the results of a numerical simulation taking into account solely the micromechanical aspect of the problem. This computation was run by means of a simple finite-difference method on the basis of two essential ingredients: (i) the intrinsic constitutive equation of the material and (ii) the two-dimensional internal stress distribution generated by the propagating band.

Basic assumptions of the model

The calibrated part of the shear specimen was considered as a mesh of $N=n_x \times n_y$ identically parallelogrammic elements of the same thickness (e) as the tested sample and whose faces are perpendicular to the Ox and Oy directions (*Figure 10*). Each element was referenced

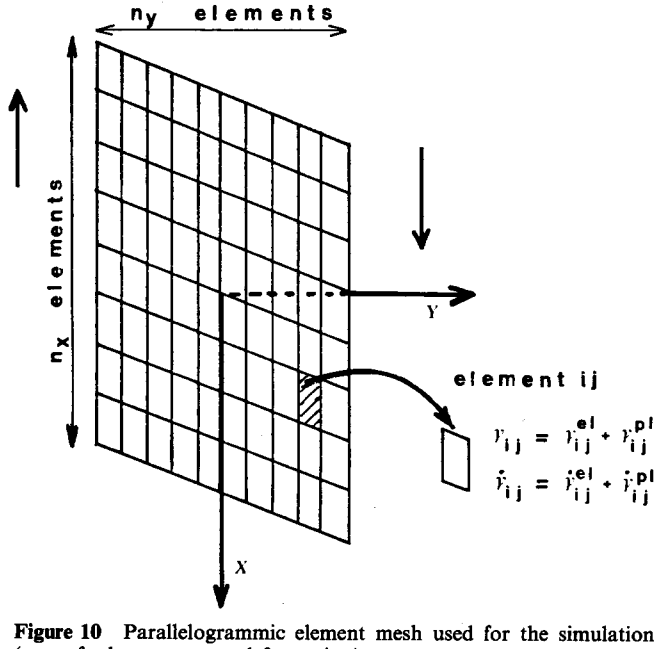

Figure 10 Parallelogrammic element mesh used for the simulation (case of a homogeneous deformation)

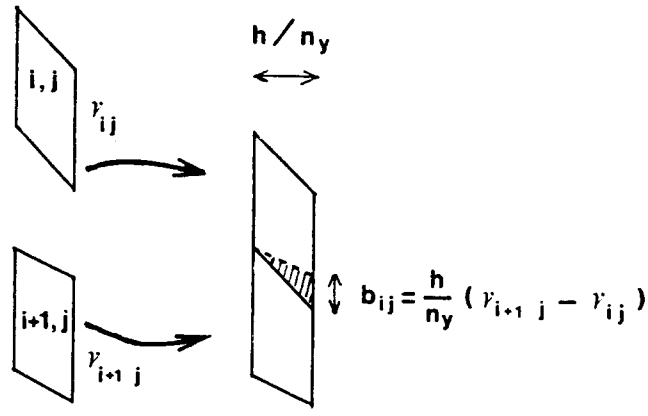

Figure 11 Induced geometrical misfit between two neighbouring elements

by its integer coordinates (i, j) in the two-dimensional array.

Following the general principle of the finite-difference scheme, it was assumed here that the strain was uniform within a given element, so that each element (i, j) corresponds to specific values of the shear $\gamma_{i,j}$ (with its elastic and plastic components, $\gamma_{i,j}=\gamma_{i,j}^{el}+\gamma_{i,j}^{pl}$) and of the shear rate $\dot{\gamma}_{i,j}$ (with $\dot{\gamma}_{i,j}=\dot{\gamma}_{i,j}^{el}+\dot{\gamma}_{i,j}^{pl}$). Owing to the plane geometry of the simple shear test, it was possible as a first approximation to take into account only the shear component of the strain tensor in view of reducing the computing time (second-order strain phenomena, like Weissenberg effect, were neglected although it was shown previously[9] that they are not completely absent in such tests).

Although the uniformity of the strain in a given element does not pose any problem if the general strain distribution is itself uniform, a geometrical misfit arises if consecutive elements along the shear axis Ox exhibit different amounts of shear, $\gamma_{i,j}$ and $\gamma_{i+1,j}$ (*Figure 11*). The amplitude of the displacement misfit is:

$$b_{i,j}=(\gamma_{i+1,j}-\gamma_{i,j})h/n_y$$

and should be accommodated by a variation of the strain within the two neighbouring elements. In the present method, however, this strain variation was not introduced explicitly but the misfit was taken into account by superimposing an internal shear stress $\tau_{int}(x, y)$ onto the uniformly applied shear stress τ. In the particular geometry of the simple shear specimen, the internal stress field caused by a shear misfit can be readily evaluated[11,19] by considering that the misfit is equivalent to a finite edge dislocation parallel to the Oz axis, with a Burgers vector $b_{i,j}$ along the Ox axis. It is well known[20] that such a perturbation induces in the surrounding medium a stress field whose shear stress component is given by the expression:

$$\tau^{int}(x, y)=\frac{\mu b(x_b, y_b)}{2\pi(1-\nu)}\frac{(x-x_b)[(x-x_b)^2-(y-y_b)^2]}{[(x-x_b)^2+(y-y_b)^2]^2} \quad (3)$$

where μ and ν are respectively the shear modulus and Poisson's ratio of the material, $b(x_b, y_b)$ is the Burgers vector at the location (x_b, y_b) of the misfitted pair of elements, while x and y are the current coordinates in the medium. In this first version of the model, we did not take into account the normal components σ_{xx} and σ_{yy} of the internal stress field, whose influence on the

plastic shear regime of polycarbonate was recognized as a second-order effect[9].

In contrast to the longitudinal shear gradients, the transverse gradients do not cause any topological misfit in the simple shear geometry, nor do they cause any specific stresses. This remark justifies the occurrence of the sharp shear band whose border marks the limit between the plastically deformed material elements within the band and the neighbouring elements, which have been subjected only to small viscoelastic strains.

The applied shear stress τ and shear γ were related to the elementary (local) stress $\tau_{i,j}$ and shear $\gamma_{i,j}$ in the following way. As concerns strains, the applied shear was obtained by averaging the local shear over the whole specimen:

$$\gamma = \langle \gamma_{i,j} \rangle = \frac{1}{N} \sum_{i=1}^{n_x} \sum_{j=1}^{n_y} \gamma_{i,j} \tag{4}$$

This formulation is justified by the geometry of the specimen, whose massive heads impose a uniform displacement on the elements lying along the extreme longitudinal rows. Concerning the stresses, the shear force was assumed to be transmitted uniformly across the width of the sample. This assumption has often been applied in previous papers[21]. It is allowed by the very slow shear rate adopted in these tests, which makes the inertia effects negligible. Furthermore, for a sample of uniform thickness, the average shear stress along a given longitudinal row of elements is equal to the applied shear stress. This latter property is specific to the symmetry of the specimens considered here, which makes the average value of the internal shear stress zero along any given longitudinal row of elements. In addition, the effect of the geometric defect was taken simply into account by an amplification of the local stress by a factor $e/e_{i,j}$, where e and $e_{i,j}$ are the nominal and defected thickness of the sample, respectively. Following the above treatment, the elementary (local) stress was computed by the relation:

$$\tau_{i,j} = \left(\frac{e}{e_{i,j}}\right)\tau + \tau_{i,j}^{\text{int}} \tag{5}$$

It is clear that, in longitudinal rows containing defect elements, the above expression does not make the average stress $\langle \tau_{i,j} \rangle$ rigorously equal to the applied stress τ. Nevertheless, it was maintained in this form for the present purpose owing to the very small reduction of thickness (1%) and the limited area of the defect introduced.

Computing algorithm

The logic scheme of the main loop of the simulation is summarized in *Figure 12*. The terms between square brackets are referred to each element (i, j) of the mesh.

At the beginning of the loop, a tentative shear stress τ is applied to the overall specimen. The shear stress field $\tau_{i,j}$ is calculated by means of relation (5), which takes into account the thickness defect of the sample and the internal stress field (equal to zero at the beginning of the simulation). Then the plastic strain field $\gamma_{i,j}^{\text{pl}}$ is computed from the total shear strain field and from the elastic shear strain field (Young's modulus and the shear stress field being known). By use of the constitutive equation (relation (1)), it is possible to determine the plastic shear-rate field $\dot{\gamma}_{i,j}^{\text{pl}}$. At this moment, the time increment

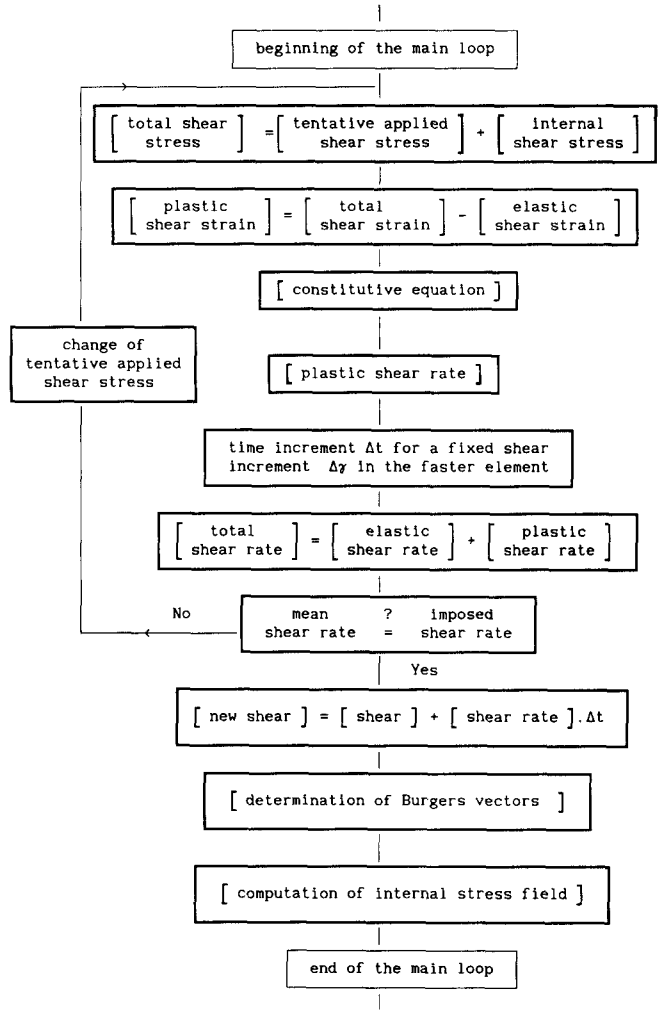

Figure 12 Logic scheme of the main loop for the simulation

is automatically computed as the time necessary to reach an imposed shear increment $\Delta\gamma_{\text{loc}}$ in the fastest element. The total shear-rate field can thus be computed by adding its plastic and elastic components.

If the comparison test between the mean calculated shear rate and the imposed shear rate of the simulation is verified, the program is continued by updating the current shear strain field, the Burgers vectors field and finally the internal stress field (by summation on overall specimen of elementary internal stress following relation (3)). In the opposite case (negative comparison test) the tentative shear stress is modified and the internal loop is followed again.

Simulation results

Figure 13 shows a simulated shear stress–shear strain behaviour during a simple plane shear test run at 25°C with a shear rate $\dot{\gamma} = 5 \times 10^{-4}\,\text{s}^{-1}$. The four successive stages of the experimental curve (*Figure 2*) are correctly taken into account by the simulation: (i) the homogeneous viscoelastic response ending at the upper yield stress (about 40 MPa), (ii) the drop of shear stress corresponding to the initiation of a shear band and its elongation, (iii) the plateau (stage III) with the lateral widening of the band and (iv) the homogeneous plastic deformation stage, which starts when the plastic zone has reached the edges of the calibrated part of the

specimen. The corresponding steps of the band propagation obtained by the computer simulation are displayed in *Figure 14*. The five upper sketches are the calculated shapes of an array of parallel lines for different values of γ (respectively 0.05, 0.15, 0.20, 0.25 and 0.55—see open circles in *Figure 13*). The first profile (*Figure 14a*) is obtained during the viscoelastic stage. The two following ones (*Figures 14b* and *14c*) show the initiation and the elongation of the band, respectively. On *Figure 14d*, the longitudinal propagation of the band is completed and finally, for $\gamma = 0.55$, the lateral widening is nearly achieved (*Figure 14e*). For a better view, the band development is shown in another representation on the five lower sketches, where the region where the local shear is greater than 0.4 was shaded in order to outline the shape of the shear-band front. The last drawing (*Figure 14e*, lower) is of particular interest. It shows that the profile of the band does not correspond, rather surprisingly, to a straight front propagation. Despite the overall symmetry of the system, it appears that the lateral widening of the band proceeds by the activation of localized sheared ledges on both its fronts. A similar conclusion has been drawn previously in an experimental and theoretical investigation on the Lüders band front in mild steels[22]. In contrast to statements generally accepted in the current literature, the authors demonstrated from microscopic observations and modelled by means of an elastic–plastic finite-element calculation that the oblique Lüders band, which is nucleated under uniaxial tension in steel, grows at the lower yield point by the activation of microscopic ledges. They found that the local microgeometry of the front induced an interfacial stress

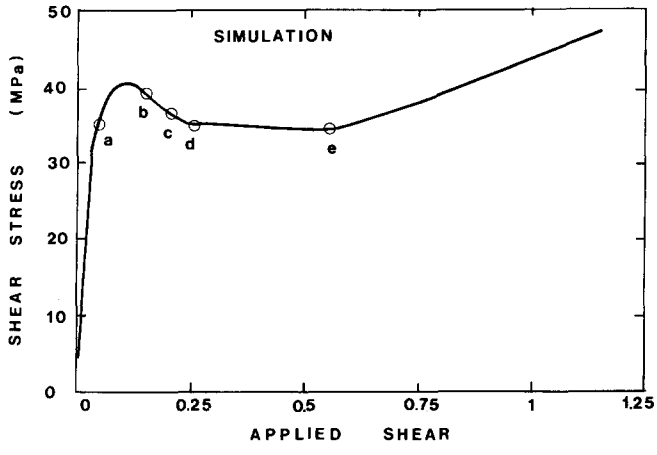

Figure 13 Applied stress–strain behaviour in a simulated simple plane shear test for $\dot{\gamma} = 5 \times 10^{-4}$ and $T = 25°C$ (open circles indicate the steps illustrated in *Figure 14*)

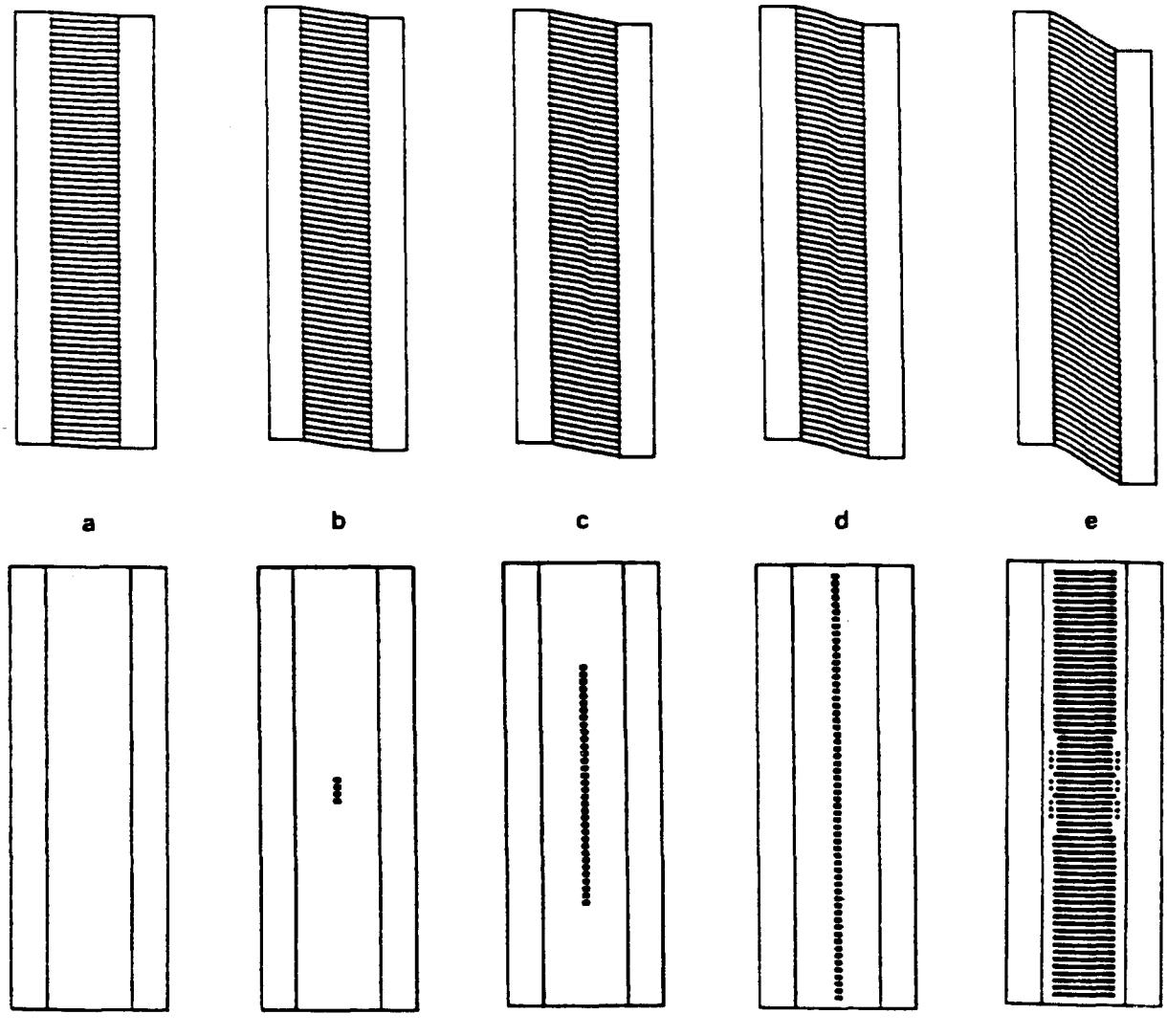

Figure 14 Computer simulation of evolution of shape of markers (upper) and of band propagation (lower): (a) $\gamma = 0.05$; (b) $\gamma = 0.15$; (c) $\gamma = 0.20$; (d) $\gamma = 0.25$; (e) $\gamma = 0.55$

concentration of the order of 1.5. It is clear that these results reported in steel are in the same vein as those described in this paper. However, in the present work, the simpler loading geometry and the non-crystalline nature of the materials emphasize the intrinsic micromechanical aspect of the band propagation process. Unlike the case of steel, where the size of ledges on the band front were found to be of the same order of magnitude as the grain diameter, the irregular shape of the front in our modelling has, evidently, no relation to any structural features since the material is amorphous. It is more likely that the size of the ledges nucleated on the band front in the polycarbonate shear specimens is related to the overall geometry of the sample, to the size of the initial defect and to the constitutive relation of the material. A quantitative correlation of these parameters would require simulation of the micromechanical process by a somewhat finer element array than that adopted in the present study. This is the aim of a further development of this work, now in progress.

SUMMARY AND CONCLUSIONS

Plane simple shear tests were performed on polycarbonate specimens with a miniaturized shearing machine, especially designed to be installed on the stage of a microscope. By means of precise *in situ* measurements (band length, band width and local shear), it was shown that, during a test, considerable shear gradients take place at the tip and on the lateral fronts of the shear band. A computer simulation was carried out on the simple hypotheses of (i) a constitutive equation and (ii) an internal shear stress field generated by the shear gradients. This modelling takes into account correctly the nucleation and the propagation of the shear band and shows that, in the plastic response of glassy polymers at large strains, the micromechanical effects play a major role in the propagation kinetics of localized shear bands, during the longitudinal development of the band and in the course of its lateral widening as well.

ACKNOWLEDGEMENTS

The authors would like to thank Mr J. M. Hiver for the quality of the SEM photographs.

REFERENCES

1 Bauwens-Crowet, C. and Bauwens, J. C. *Polymer* 1983, **24**, 921
2 Bauwens-Crowet, C., Ots, J. M. and Bauwens, J. C. *J. Mater. Sci.* 1974, **9**, 1197
3 Brady, T. E. and Yeh, C. S. Y. *J. Appl. Phys.* 1971, **42**, 4622
4 G'Sell, C. and Gopez, A. J. *J. Mater. Sci.* 1985, **18**, 3462
5 Wu, W. and Turner, A. P. L. *J. Polym. Sci.* 1973, **11**, 2199
6 Bowden, P. B. and Jukes, J. A. *J. Mater. Sci.* 1972, **7**, 52
7 Chau, C. C. and Li, J. C. *J. Mater. Sci.* 1979, **14**, 2172
8 Shrivastava, S. C., Jonas, J. J. and Canova, G. *J. Mech. Phys. Solids* 1982, **30**, 75
9 G'Sell, C., Boni, S. and Shrivastava, S. *J. Mater. Sci.* 1983, **18**, 903
10 El Bari, H. Doctoral Thesis, INPL, Nancy, 1987
11 G'Sell, C. in 'Strength of Metals and Alloys', (Eds. H. J. McQueen *et al.*), Pergamon Press, Oxford, 1986, p. 1943
12 G'Sell, C., Perez, J., Cavaille, J. Y., El Bari, H. and Johari, G. P. *Mater. Sci. Eng. (A)* 1989, **110**, 223
13 Parisot, J., Rafi, O. and Choi, W. J. *Polym. Eng. Sci.* 1984, **24**, 886
14 Argon, A. S. *Phil. Mag.* 1973, **28**, 839
15 G'Sell, C. and Jonas, J. J. *J. Mater. Sci.* 1979, **14**, 583
16 Bowden, P. B. *Phil. Mag.* 1970, **22**, 455
17 Li, J. C. M. in 'Plastic Deformation of Amorphous and Semi-crystalline Materials', (Eds. B. Escaig and C. G'Sell), Les Editions de Physique, Paris, 1982, p. 29
18 G'Sell, C. *Rev. Phys. Appl.* 1988, **23**, 1085
19 Bowden, P. B. and Raha, S. *Phil. Mag.* 1974, **29**, 149
20 Hirth, J. P. and Lothe, J. 'Theory of Dislocations', Wiley, Chichester, 1982
21 G'Sell, C., Aly Helal, N. A. and Jonas, J. J. *J. Mater. Sci.* 1983, **18**, 1731
22 Iricibar, R., Mazza, J. and Cabo, A. *Acta Metall.* 1977, **25**, 1163